Molecular Therapy
Nucleic Acids
Original Article

A Simple System for Differentiation of Functional Intestinal Stem Cell-like Cells from Bone Marrow Mesenchymal Stem Cells

Lei Ye,[1,3] Lei X. Sun,[2,3] Min H. Wu,[1] Jin Wang,[2] Xin Ding,[2] Hui Shi,[1] Sheng L. Lu,[2] Lin Wu,[1] Juan Wei,[1] Liang Li,[2] and Yu F. Wang[1]

[1]Department of Gastroenterology and Hepatology, Jinling Hospital, Medical School of Nanjing University, 305 Zhongshan East Road, Nanjing 210002, Jiangsu Province, China; [2]State Key Laboratory of Pharmaceutical Biotechnology, Jiangsu Engineering Research Center for MicroRNA Biology and Biotechnology, NJU Advanced Institute for Life Sciences, School of Life Sciences, Nanjing University, 163 Xianlin Road, Nanjing, Jiangsu 210023, China

Disruption of normal barrier function is a fundamental factor in the pathogenesis of inflammatory bowel disease, and intestinal stem cell (ISC) transplantation may be an optional treatment for patients. However, it is complicated and inefficient to isolate ISCs from the intestine, which hampers its wide application in clinic. We developed a two-step protocol in which mesenchymal stem cells (MSCs) were first induced into Sox17- or Foxa2-positive definitive endoderm cells by activin A treatment and then into Lgr5-positive ISC-like cells by miR-17 and FGF2 treatment. Furthermore, these Lgr5-positive cells could differentiate into enterocyte-like cells following induction with EGF. The results from an *in vivo* experiment showed that the MSC-derived Lgr5-positive cells were able to protect against dextran sulfate sodium-induced colitis. Taken together, our work might provide a new source of autologous ISCs.

INTRODUCTION

Inflammatory bowel disease (IBD) is characterized by chronic inflammation in the gut and periods of remission, as well as intermittent relapses. Although anti-tumor necrosis factor (TNF) agents like infliximab (IFX) and adalimumab (ADA) have greatly improved the clinical symptoms and endoscopically viewed bowel ulcerations, there remain a substantial group of patients whose clinical course cannot be adequately controlled.[1,2] The intestinal epithelium is restored by multipotent intestinal stem cells (ISCs). ISCs reside in crypts and differentiate into epithelial cells as they move from the crypt base to the villous tip.[3] Thus, ISCs are critical in maintaining the absorptive function of the intestine. It is reasonable to hypothesize that ISC transplantation would benefit patients with IBD. However, ISC transplantation is impractical in the clinic because isolating ISCs from the crypts is technically complicated, and each crypt contains only 6–10 ISCs.[4]

Decades of research into specific genetic markers of ISCs have facilitated their isolation from other crypt-based cell types. The G protein-coupled receptor Lgr5, the RNA-binding protein Musashi-1, and the polycomb group protein Bmil have recently been described as molecular markers of ISCs.[5–8] Spence et al.[9] have reported an efficient way to direct the differentiation of human pluripotent stem cells (hPSCs) into intestinal tissue *in vitro*. However, three-dimensional organoids are formed in a three-dimensional culture supplemented with large quantities of growth factors, which is costly and may not be suitable for clinical practice. Therefore, a monolayer system that can differentiate the stem cells into intestinal cells is urgently needed. Several studies have demonstrated protocols that can successfully direct the differentiation of hPSCs or embryonic stem cells (ESCs) into intestinal epithelial cells.[10–12] Nevertheless, the efficiency of inducing somatic cells into PSCs is unsatisfactory. In addition, it is widely accepted that both PSCs and ESCs have a relatively high risk for neoplasia.[13]

In contrast with PSCs, mesenchymal stem cells (MSCs) can be isolated from a variety of tissues, such as bone marrow, placenta, and umbilical cord.[14] The biological functions of bone marrow-derived MSCs (BM-MSCs) have been best characterized, and they are most widely used for immunoregulation and regenerative cell therapy.[15–17] However, there has not yet been a study exploring the efficiency of MSC differentiation into ISCs. It has been confirmed that intestinal epithelium is derived from the definitive endoderm (DE), which could be induced by activin A.[18,19] Regionalization occurs along the anterior-posterior axis of the DE.[20] The expression of specific transcription factors marks the regionalization of DE. Sox17- or Foxa2-positive DE represents posterior endoderm that

Received 21 February 2018; accepted 19 August 2018;
https://doi.org/10.1016/j.omtn.2018.08.017.

[3]These authors contributed equally to this work.

Correspondence: Yu F. Wang, Department of Gastroenterology and Hepatology, Jinling Hospital, Medical School of Nanjing University, 305 Zhongshan East Road, Nanjing 210002, Jiangsu Province, China.
E-mail: wangfy65@nju.edu.cn
Correspondence: Liang Li, State Key Laboratory of Pharmaceutical Biotechnology, Jiangsu Engineering Research Center for MicroRNA Biology and Biotechnology, NJU Advanced Institute for Life Sciences, School of Life Sciences, Nanjing University, 163 Xianlin Road, Nanjing, Jiangsu 210023, China.
E-mail: lijing@sibs.ac.cn

could develop into hindgut, which could later give rise to the small and large intestine.[21–23] Recently, it has been demonstrated that treatment with a high concentration of fibroblast growth factor 2 (FGF2; 256 ng/mL) was able to specify ESC-derived DE into anterior foregut and small-intestinal cells.[24]

MicroRNAs (miRNAs) have been well investigated in a variety of physiological and pathophysiological processes. It has been reported that miR-17 might play an important role in the embryonic development of the colonic epithelium.[25] High expression of miR-17 was found in early embryonic colon tissue, but its expression decreased as colon embryonic development progressed.[25] Moreover, overexpression of miR-17-5p in the crypt progenitor compartment was confirmed by *in situ* hybridization.[25] Hence the aim of the study was to investigate whether BM-MSCs could be efficiently differentiated into ISC-like cells under the mediation of miR-17, activin A, and FGF2, and to further explore the functions of the MSC-derived stem cells *in vivo*.

RESULTS

Stepwise Differentiation of BM-MSCs toward ISC-like Cells

Morphologically, BM-MSCs of passage 3 appeared to be a homogeneous population of spindle-shaped cells. Almost all MSCs expressed the bone marrow progenitor cell marker CD29, and most cells expressed CD106 and CD90. Seldom did BM-MSCs express CD45 and CD3 (Figure 1A). These cells were used in subsequent experiments.

It has been demonstrated that activin A could promote DE formation by activating the nodal and activin signaling pathway.[19] However, the concentrations of activin A used were different among the published work.[12,19] Thus, the first step was to determine the optimal concentration of activin A. Different concentrations of activin A (0, 1, 5, 10, 20, and 100 ng/mL) were used to treat BM-MSCs for 5 days. We found that the expression of DE-specific genes was significantly upregulated on day 5. Maximal expression of DE-related genes (Sox17 and Foxa2) was observed with 5 ng/mL activin A treatment (Figure 1B). Western blot analysis of Sox17 and Foxa2 expression also confirmed these findings (Figure 1C). In the immunofluorescence assay, we randomly selected six fields, counted the number of positive and negative cells, and then calculated the percentage. The average proportions of Sox17-positive and Foxa2-positive cells were approximately 76.76% and 78.58%, respectively, on day 5 following treatment with 5 ng/mL activin A (Figure 1E). Furthermore, Foxa2 and Sox17 proteins were expressed in the nuclei (Figure 1D). Wnt3a has been reported to have synergistic effects with activin A in the induction of DE cells from MSCs; but in our study, Wnt3a did not increase the number of Sox17- and Fox2-positive cells (data not shown).[19,26]

Then the DE cells were subsequently induced into ISC-like cells by FGF2. Lgr5 and Musashi-1 are two proteins that could be considered as markers of ISCs.[5,7,8] As shown in Figure 2A, the expression of Lgr5 and Musashi-1 genes was markedly elevated in a time-dependent manner. Maximal expression was observed after 250 ng/mL of FGF2 treatment for 4 days. Western blot also showed that the maximal expression of Lgr5 and Musashi-1 genes occurred on day 4 (Figure 2C). However, immunofluorescence staining revealed relatively weak fluorescence intensity and only a small proportion of Lgr5-positive cells (Figure 2B). The results from flow cytometry assays confirmed that the proportion of Lgr5-positive cells was only 30.06%, which indicated the low efficiency of the induction protocol (Figure 2D). Besides, human BM-MSCs were used to explore whether the two-step protocol was also applicable. It indicated that human BM-MSCs could also express the protein of Lgr5, although the positive proportion was lower than that of rat BM-MSCs (Figure 2E).

miR-17 Facilitates the Differentiation of DE Cells Toward ISC-like Cells by Activating the Wnt/β-Catenin Pathway

To investigate whether miR-17 is critical in the differentiation process, we used qRT-PCR to measure the expression of miR-17 throughout the whole protocol. As shown in Figure 3A, the expression of miR-17 gradually increased in the first 5 days. During the induction of DE cells into ISC-like cells, the expression of miR-17 reached a peak for a short time and then quickly diminished thereafter. Hence DE cells were infected with a lentiviral system expressing miR-17, and qRT-PCR confirmed the successful overexpression of miR-17 in DE cells (Figure 3B). The expression of Lgr5 and Musashi-1 genes was also measured using qRT-PCR, and the results showed that mRNA expression of these two genes was markedly higher in cells treated with both miR-17 and FGF2 than in cells treated with FGF2 only. Moreover, their expression levels peaked on day 2, not day 4 (Figure 3D). Then western blot was used to measure the protein expression of the two markers on day 2 following the mediation of miR-17 and FGF2. The result was consistent with that of qRT-PCR (Figure 3C). The immunofluorescence assay revealed stronger fluorescence intensity and a greater proportion of Lgr5-positive and Musashi-1-positive cells in cells treated with both miR-17 and FGF2 than in cells treated with only FGF2 (Figure 3E). Flow cytometry assays reported that the proportion of Lgr5-positive cells reached as high as 89.14% (Figure 3F). These results fully demonstrated the synergistic role of miR-17 in inducing DE cells toward an ISC-like cell fate. Next, we sought to explore the mechanisms underlying the phenomenon.

The Wnt/β-catenin pathway has been reported to play an important role in intestinal morphogenesis.[27,28] In their work, Ogaki et al.[10] showed that Wnt signaling was necessary for the differentiation of ESCs into intestinal lineages *in vitro*. Thus, we speculated that miR-17 could activate the Wnt/β-catenin pathway. WIF1 and E2F1 are two potent Wnt pathway antagonists.[29,30] To explore whether the Wnt/β-catenin pathway was involved in the effects of miR-17 on DE cell differentiation, the protein levels of P-β-catenin, β-catenin, E2F1, and WIF1 were detected *in vitro* 2 days after miR-17 transfection. The results indicated that miR-17 caused a significant reduction in the phosphorylation of β-catenin, WIF1, and E2F1. However, the total protein levels of β-catenin remained unchanged (Figure 4A). To further investigate whether WIF1 and E2F1 were the direct downstream targets of miR-17-5p, we cloned the 3′ UTR and targeting sites

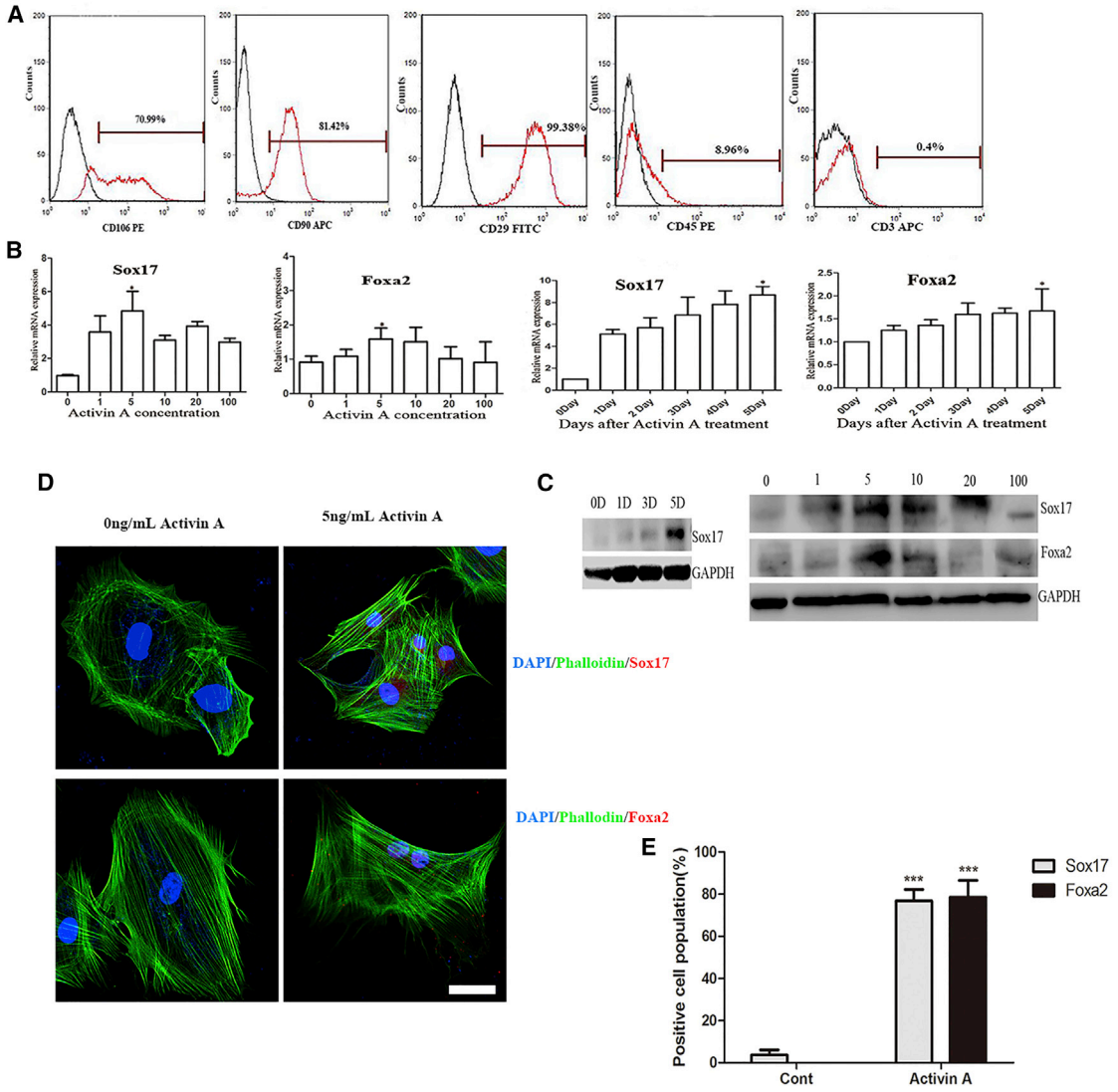

Figure 1. BM-MSCs Could Be Induced to Form Definitive Endoderm by Activin A

(A) Flow cytometric analysis of BM-MSCs at passage 3. The analysis showed a predominant population of cells that were positive for CD106, CD90, and CD29, and negative for CD45 and CD3. (B and C) Passage 3 BM-MSCs were stimulated with different concentrations of activin A (0, 1, 5, 10, 20, and 100 ng/mL) for 5 days, and the expression levels of the definitive endoderm markers Sox17 and Foxa2 were analyzed by qRT-PCR (B) and western blot (C). The results were calculated by normalizing to those in the day 5 untreated MSCs. Data are shown as the mean ± SEM; n = 3. *$p < 0.05$. (D) Immunofluorescence images of Foxa2- or Sox17-positive cells after BM-MSCs treated with 5 ng/mL activin A for 5 days. Nuclei were stained with DAPI. Phalloidin could specifically bind to Actin and help present cytoskeleton. Scale bar: 50 μm. (E) A statistic summary of Sox17- or Foxa2-positive cell proportions. Data are shown as the mean ± SEM; n = 6. ***$p < 0.001$.

of WIF1 and E2F1 mRNA into pMIR-REPORT Luciferase plasmid. The construct was cotransfected into 293T cells along with miR-17-5p. The precursor significantly reduced the luciferase activity driven by the wild-type 3′ UTR of WIF1 and E2F1 compared with miR-NC in 293T cells. Meanwhile, the luciferase activities of cells expressing the mutated-type WIF1 and E2F1 3′ UTR and empty vector were not inhibited by the miR-17-5p precursor. These results confirmed that WIF1 and E2F1 were the direct targets of miR-17-5p (Figures 4B and 4C).

The above data indicated that the simultaneous application of miR-17 and FGF2 dramatically increased the expression of ISC markers by activating canonical Wnt/β-catenin signaling. Next, to determine whether the induced ISC-like cells were capable of differentiating into intestinal epithelial cells *in vitro*, we recultured the induced cells with 20 ng/mL epidermal growth factor (EGF) for another 16 days. The expression of enterocyte molecular markers (ISX, DDP4, and villin 1) was induced, as revealed by qRT-PCR[12] (Figure 4E). Immunocytochemical analysis showed that the induced enterocytes also

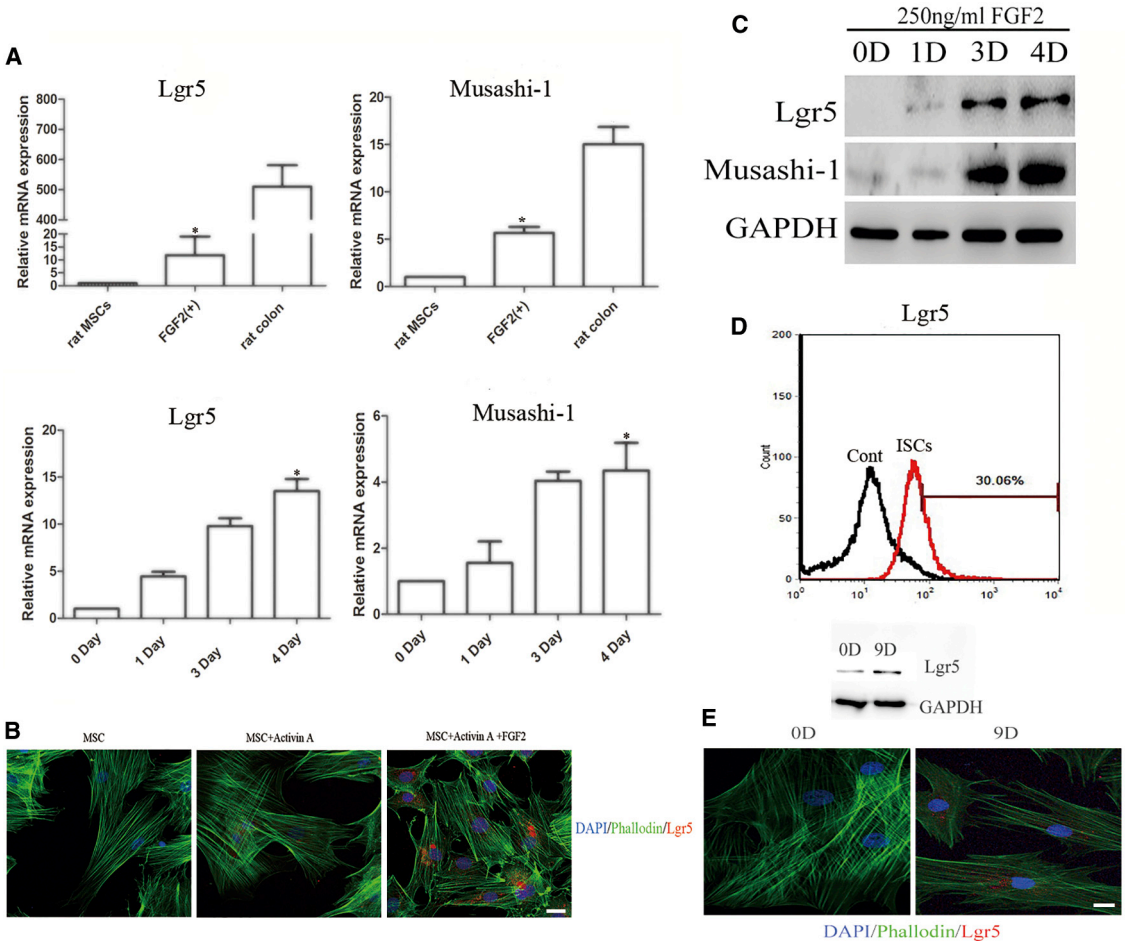

Figure 2. Characterization of BM-MSC-Derived Intestinal Stem Cell-like Cells by Stepwise Differentiation

(A) Expression levels of the intestinal stem cell markers Lgr5 and Musashi-1 were analyzed by qRT-PCR. The results were calculated by normalizing to those in the day 9 untreated MSCs. Data are shown as the mean ± SEM; n = 3. *$p < 0.05$. (B) Immunofluorescence analysis of the dynamic change of Lgr5-positive cells during differentiation. Nuclei were stained with DAPI. Scale bar: 50 μm. (C) Dynamic protein expression of Lgr5 and Musashi-1 was analyzed by western blot. (D) The proportion of Lgr5-positive cells after 250 ng/mL FGF2 treatment for 4 days was analyzed by flow cytometry analysis. (E) Western blot and immunofluorescence showed that human BM-MSCs could be induced to express the protein Lgr5 by treatment with 5 ng/mL activin A for 5 days and then 250 ng/mL FGF2 for 4 days. Nuclei were stained with DAPI. Scale bar: 50 μm.

expressed Muc2, CK-18, and E-cadherin[10] (Figure 4D). Moreover, we also confirmed that MSC-derived enterocytes could absorb β-Ala-Lys (AMCA), a fluorescent dipeptide, which indicated that the induced enterocytes expressed the enterocyte-specific transporter PEPT1[11] (Figure 4F). Taken together, all of these results revealed that exogenous miR-17 greatly enhanced the expression of ISC markers via the activation of the Wnt/β-catenin pathway and the reduction of WIF1 and E2F1 levels. Our protocol was summarized in Figures 4G and 4H.

ISC-like Cells Rescue Damaged Epithelium

To test the therapeutic potential of ISC-like cells, we established an animal model of colonic mucosal damage by feeding BALB/c 3% dextran sulfate sodium (DSS) for 7 days.[31] Most of the mice developed acute colitis, which was characterized by weight loss, bloody stool, and diarrhea. At 7 and 9 days after initiating DSS administration, we instilled the induced ISCs by enema into the recipient mice. The whole transplantation protocol was shown in Figure 5A. DSS+ISC-treated mice showed significantly reduced weight loss and faster body weight recovery compared with DSS+PBS-treated mice from day 8 to the end of the observation period (Figure 5B, with statistically significant differences on days 9, 10, 11, and 12; $p < 0.05$). Colitis was correlated with colon damage and inflammation, which were characterized by colon shortening and higher inflammatory cytokine levels. A significant decrease in colon shortening was observed in the DSS+ISC-treated mice (Figure 5C). Histopathological examination of the distal colon section showed that ISC treatment significantly reduced the severity of epithelial damage and inflammatory cell infiltration compared with DSS-treated mice that received only PBS (Figure 5D). We next investigated the *in vivo* effect of ISCs on the

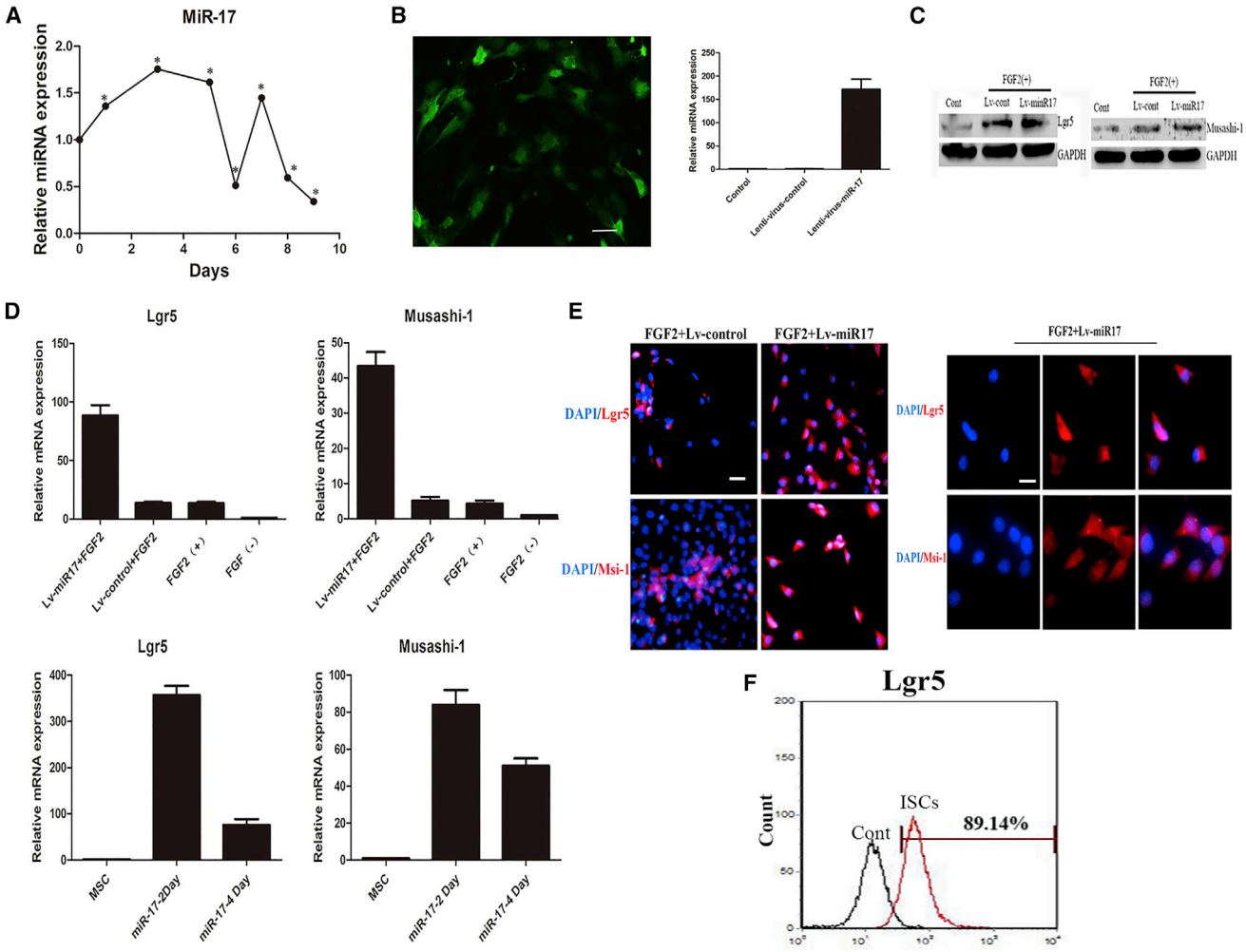

Figure 3. miR-17 Worked Cooperatively with FGF2 to Drive BM-MSCs Toward Intestinal Stem Cell-like Cells

(A) The expression of miR-17 was measured throughout the whole protocol (MSCs were induced into endoderm by activin A and then were subsequently induced into ISC-like cells by FGF2). The results were calculated by normalizing to those untreated MSCs. Data are shown as the mean ± SEM; n = 3. *p < 0.05. (B) qRT-PCR confirming induced overexpression of miR-17. Gene expression levels of miR-17 were analyzed by qRT-PCR. The results were calculated by normalizing to endoderm cells without transfection. Data are shown as the mean ± SEM; n = 3. Scale bar: 100 μm. (C) Western blot analysis of cells infected with Lenti-miR-1 or Lenti-NC. (D) Gene expression levels of Lgr5 and Musashi-1 were analyzed by qRT-PCR. The results were calculated by normalizing to those in the day 9 untreated endoderm cells (above figures) or in the nine untreated MSCs (below figures). Data are shown as the mean ± SEM; n = 3. (E) Immunofluorescence staining of Lgr5 and Musashi-1 in Lenti-miR-17-transfected cells. Nuclei were stained with DAPI. Scale bars: 25 μm (left); 12.5 μm (right). (F) The proportion of Lgr5-positive cells following treatment with miR-17 and FGF2 for 2 days was analyzed by flow cytometry.

production of inflammatory mediators that were presumed to be downregulated. The colons of ISC-treated mice contained reduced levels of inflammatory cytokines (interferon-γ [IFN-γ], interleukin-10 [IL-10], IL-6, and TNF-α) (Figure 5E). We also determined the plasma levels of IFN-γ, IL-10, IL-6, IL-1β, and TNF-α. The results showed that ISC treatment could reduce the systemic inflammatory responses in DSS-treated mice (Figure S1).

The Swiss roll technique revealed that multiple GFP^+ areas were concentrated in the middle and lower parts of the colon, which were the most severe sections of the induced colitis model (Figure S2). GFP^+ cells could migrate to the inflamed areas. Figure 6E showed that parts of crypts and the epithelium were surrounded by neutrophils marked by CD11b, and GFP^+ cells could be observed in these areas. They moved through the gut tract, and some of them formed flat or slightly invaginated linings, connecting to the recipient colon epithelium (Figures 6C and 6D). Below the epithelium surface, GFP^+ cells were also observed in the cystic areas (Figures 6A and 6B). The higher magnification view was shown in Figure S3. The migration process was captured by confocal microscopy (Figure S4). Four weeks after DSS administration, the structure of the epithelium in the treated mice has recovered and appeared similar to normal

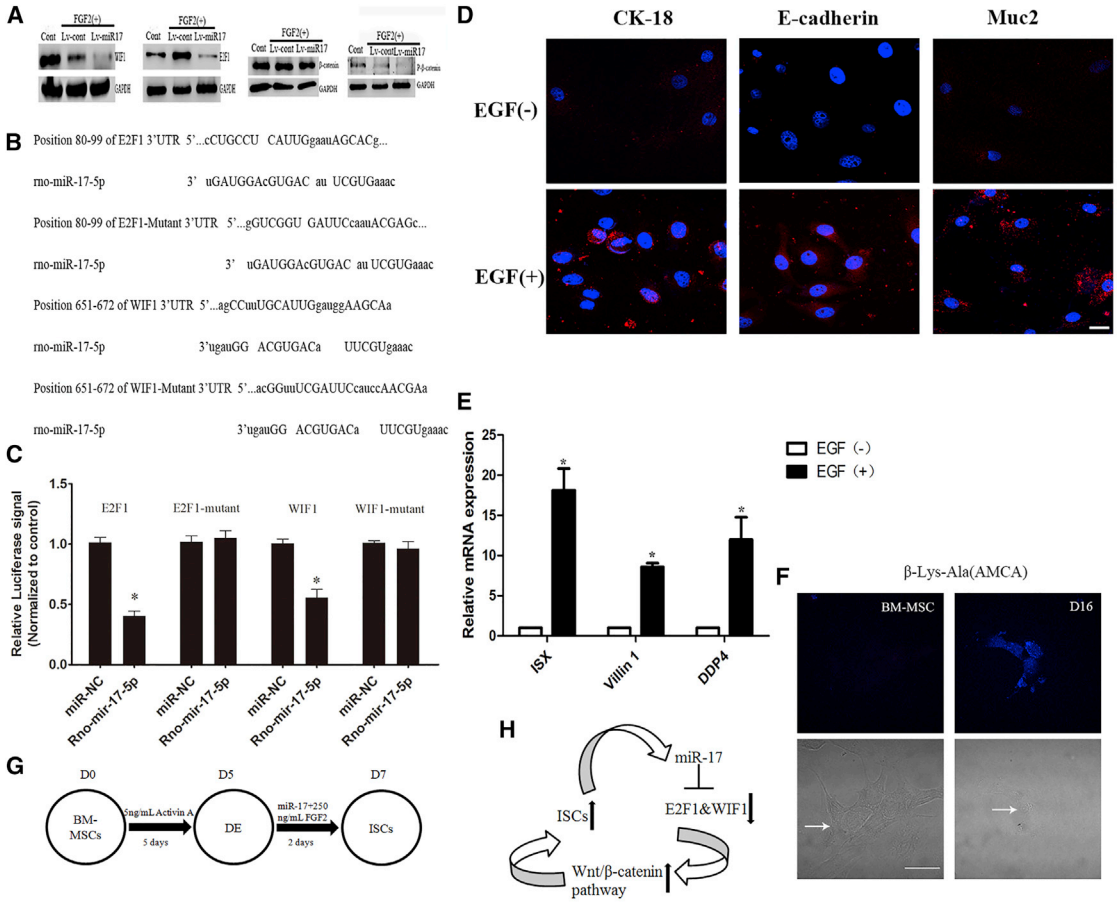

Figure 4. miR-17 Activated the Wnt/β-Catenin Signaling Pathway by Downregulating E2F1 and WIF1

(A) Western blot analysis of WIF1, E2F1, β-catenin, and P-β-catenin expression in the presence of exogenous miR-17. (B) Predicted consequential pairing of the target region of WIF1 and E2F1 with miR-17-5p. (C) Interaction of miR-17-5p with the 3′ UTR of WIF1, E2F1, WIF1 Mutant, or E2F1 Mutant, as determined by luciferase activity. *$p < 0.05$. (D and E) The induced intestinal stem cells were treated with 20 ng/mL EGF for 16 days. qRT-PCR and immunofluorescence staining confirmed the expression of epithelial cell markers (D: Muc2, CK-18, and E-cadherin; E: ISX, villin 1, DDP4). The results were calculated by normalizing to those ISC-like cells without EGF treatment for 16 days. Data are shown as the mean ± SEM; n = 3. *$p < 0.05$. Nuclei were stained with DAPI. Scale bar: 50 μm. (F) β-Lys-Ala (AMCA) intake assayed at day 16. AMCA exhibited blue fluorescent. Arrows showed the morphology of cells in a white light confocal microscope. Scale bar: 25 μm. (G and H) Differentiation protocol for the generation of definitive endoderm and intestinal stem cell-like cells from BM-MSCs (G); the signaling pathway was confirmed after miR-17 transfection (H).

morphology. Some GFP^+ cells were found in the epithelium, and the merged image shows that these cells also expressed CK-18, the marker of epithelial absorptive cells (Figure 6F), which meant that the transplanted cells could survive well in the colons of the recipients and differentiate into epithelial cells.

DISCUSSION

In the past two decades, we have seen an explosion of scientific and clinical interest in stem cell transplantation for a variety of diseases, including IBD. Compared with the accumulating studies on MSCs, there is limited literature on ISCs. The main reason is that the method to obtain ISCs is far more complicated than that to obtain MSCs. The establishment of a simple and efficient differentiation method with which to induce BM-MSCs into ISC-like cells *in vitro* seems to be a promising solution. Ogaki et al.[10] have successfully induced ESCs into intestinal lineages by activating Wnt/β-catenin and inhibiting the Notch signaling pathway. However, they failed to manipulate the differentiation of ISCs by activating the Wnt or Notch signaling pathway. Iwao et al.[12] have reported that the expression of Lgr5 has been detected in the human induced pluripotent stem cell (hiPSC) differentiation system. Nevertheless, neither the proportion of the $Lgr5^+$ cells nor whether the ISC-like cells could function well *in vivo* was reported in their work. Thus, our work is very important. We have successfully directed BM-MSCs into ISC-like cells by activating Wnt and FGF signaling. Moreover, when cultured with EGF, the $Lgr5^+$ and $Musashi\text{-}1^+$ cells could further differentiate into intestinal absorptive cells. *In vivo*, the transplanted GFP^+ ISC-like cells readily integrate into the mouse colon, covering the epithelium and residing in the crypts. At 4 weeks after DSS administration, these cells formed a single-layered

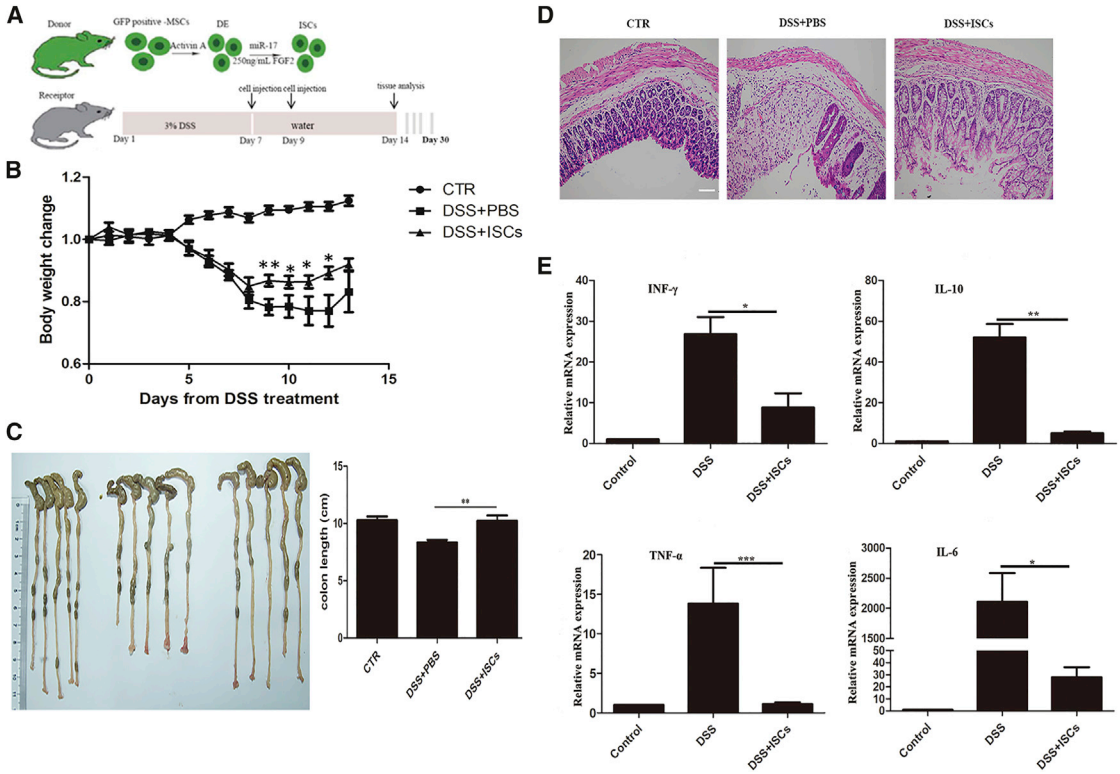

Figure 5. Treatment with Intestinal Stem Cell-like Cells Protected against DSS-Induced Colitis

(A) Experimental protocols. (B) The progression of colitis was monitored by body weight changes, which were presented as a percentage of their initial weight (day 0: 100%). CTR, healthy control mice (n = 9); DSS+ISCs, DSS-treated mice that received intestinal stem cell-like cells (n = 11); DSS+PBS, DSS-treated mice that received only PBS (n = 10). Data are shown as the mean ± SEM. *$p < 0.05$; **$p < 0.01$. (C) Macroscopic image of mouse colons harvested on day 14 and the assessment of the colonic length. The groups from left to right are CTR, DSS+PBS, and DSS+ISCs. Data are shown as the mean ± SEM. **$p < 0.01$. (D) Photomicrographs of H&E-stained paraffin sections of mouse colons harvested at day 14. A representative example of each group was shown. Scale bar: 200 μm. (E) Cytokine levels of colons were analyzed by qRT-PCR. The results were calculated by normalizing to the control group. Data are shown as the mean ± SEM; n = 5. *$p < 0.05$; **$p < 0.01$; ***$p < 0.001$.

villus that was histologically normal. Overall, these data suggest the potential of ISC therapy based on the differentiation of BM-MSCs *in vitro*.

miR-17, a member of the miR-17/92 cluster, has been shown to be a tumor promoter in many studies.[32–34] Recently, a study from Mao et al.[35] demonstrated that the miR-17/92 cluster stimulated the neuronal differentiation of neural stem cells. In addition, miR-17 has been reported to facilitate the adipogenic differentiation of BM-MSCs.[36] Here, in our MSC differentiation system, we found that miR-17 alone could greatly enhance the activity of the Wnt/β-catenin signaling pathway through downregulating its direct suppressors E2F1 and WIF1, subsequently increasing the abundance of ISC-like cells.

The simple and efficient protocol with which to direct BM-MSCs into ISC-like cells was first proposed by our team. These results revealed an important role for miR-17 and Wnt/β-catenin in posteriorizing the endoderm. FGF2 signaling works cooperatively with miR-17 to drive DE cells toward an Lgr5-expressing ISC lineage. Our study indicated that miR-17 participates in a variety of physiological and pathological processes, except for tumorigenesis. An miRNA cluster is defined as several miRNA genes located adjacent to each other on the chromosome that often, but not always, target common mRNAs, which are often present in the same pathway. Therefore, other members of the miR-17/92 cluster should also be investigated in the differentiation system.[37,38] Additionally, the long-term safety of stem cell transplantation still needs to be evaluated. MSCs have been shown to favor tumor growth due to its immunologic effects.[39,40] Therefore, the safety of long-term ISC engraftment (>6 months) should be investigated in future research.

Conclusions

In summary, our results suggest that miR-17 effectively facilitates the differentiation of BM-MSCs toward ISC-like cells through activating the Wnt/β-catenin signaling pathway. Furthermore, cultured BM-MSC-derived ISC-like cells could migrate to the damaged mucosa and help rescue the damaged epithelium by differentiating into enterocytes and alleviating intestinal inflammation. These findings support the clinical application of ISC therapy.

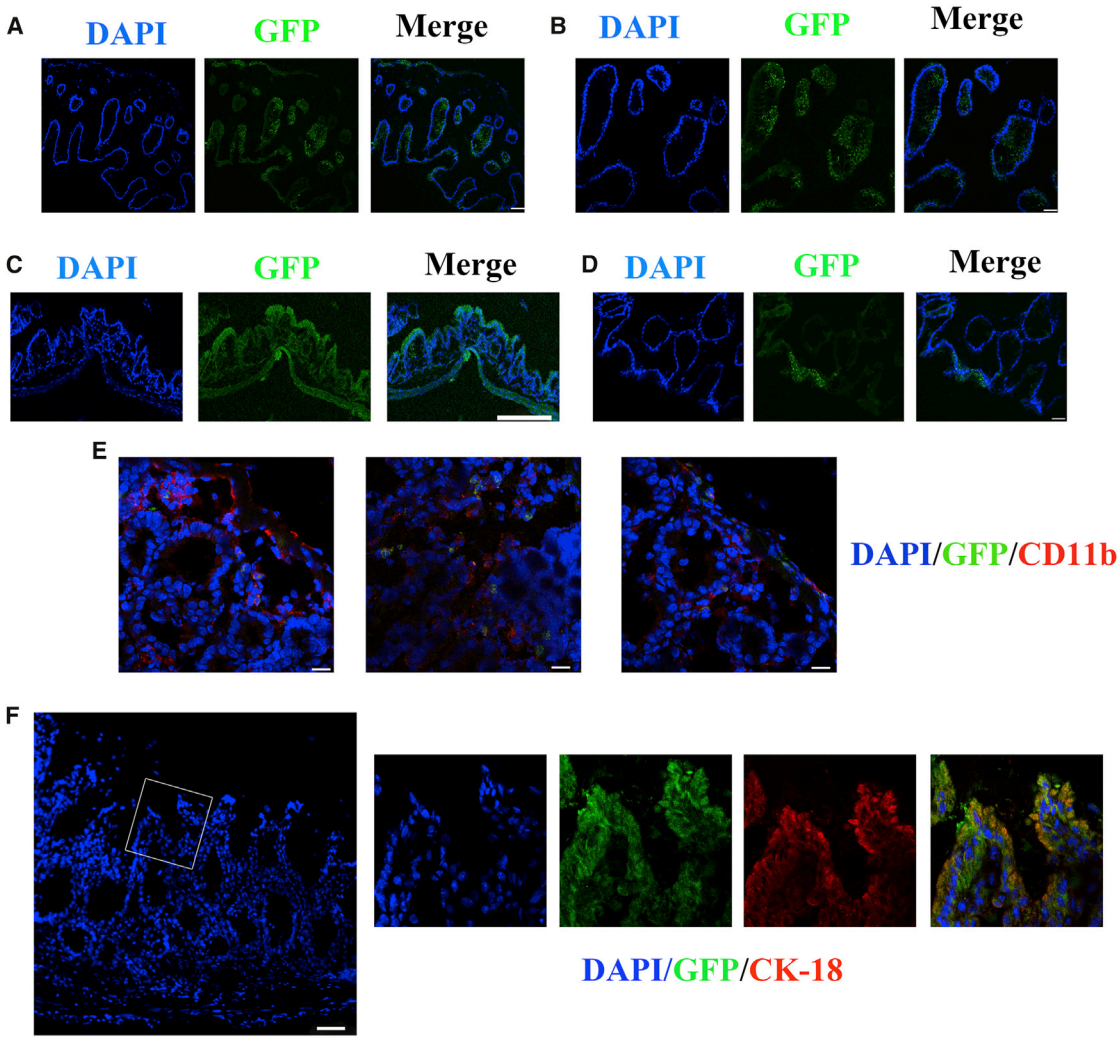

Figure 6. Recipient Colon Sections after Transplantation Were Analyzed by Confocal Microscopy

(A and B) GFP$^+$ cystic structures were observed: lower magnification (A) and higher magnification (B). (C and D) The GFP$^+$ cells forming flat linings cover the damaged mucosa: lower magnification (C) and higher magnification (D). (E) GFP$^+$ cells could migrate to the inflamed areas. Neutrophils were stained with anti-CD11b antibody. (F) One month after DSS administration, merged images show GFP$^+$ cells in the epithelium of the colon, which were positively immunostained for CK-18. Nuclei were stained with DAPI. Scale bars: 25 μm (B and D); 50 μm (E); 75 μm (A and F); 200 μm (C).

MATERIALS AND METHODS

Isolation and Culture of MSCs

Four-week-old male Sprague-Dawley rats, which were purchased from Shanghai Super–B&K Laboratory Animal, were killed by cervical dislocation, and bone marrow cells were harvested by inserting a needle into the shaft of the tibias and femurs, and flushing it with 10 mL of DMEM medium (GIBCO) supplemented with 10% fetal bovine serum (FBS) (GIBCO) and 1% penicillin and streptomycin (GIBCO). Cell suspensions were filtered through a 40-μm nylon filter and plated in 10-cm dishes. The cells were maintained in DMEM with 10% FBS at 37°C and 5% CO2. The medium was changed every 3 days. The adherent cells were passaged when the cells were ~80% confluent. Cells between passages 3 and 6 were used for experiments.

Here, we thank Prof. P.P. Shen from the Life Science School of Nanjing University for providing us with human BM-MSCs. The culture conditions of human BM-MSCs were the same with those of rat BM-MSCs.

Fluorescence-Activated Cell Sorting Analysis of MSCs

Cultured cells were subjected to fluorescence-activated cell sorting (FACS) analysis for the expression of various markers of MSCs. Cells were trypsinized, collected, and incubated in PBS with 2% BSA for 1 hr, which was followed by incubation in fluorescein-labeled anti-rat CD29, CD3,CD45, CD90, and CD10 (BD, USA) for 30 min at room temperature. The dilution was 1 μL of primary antibodies per 100 μL of PBS containing 2% BSA. After washing and resuspending

in 300 μL of PBS, the immunofluorescence signal was detected using BD FACSCalibur. A negative control was processed by incubating cells in buffer without primary antibodies.

Differentiation Program

BM-MSCs of passage 3 were seeded onto six-well plates. After adherence, the medium was changed to DMEM+1% FBS. Different concentrations of activin A (0, 1, 5, 10, 20, and 100 ng/mL) were added to the medium. Activin A was purchased from Sino Biological. After 5 days, the expression of Foxa2 and Sox17 was measured by qRT-PCR and western blot. Then the optimal concentration of activin A was used in the following experiment. For ISC-like cell differentiation, DMEM/F12 (GIBCO)+2% FBS supplemented with 250 ng/mL FGF2 (R&D Systems) was applied to the cells for 4 days. Lgr5 and Musashi-1, two ISC markers, were evaluated at the end of the protocol. To further observe whether the induced ISC-like cells could differentiate into intestinal epithelial cells, we cultured cells in DMEM/F12 containing 2% FBS and 20 ng/mL EGF (R&D systems) for 16 days. The medium was changed every 2 days.

FACS Analysis of Lgr5-Expressing MSC-Derived ISCs

MSC-derived ISCs were trypsinized and resuspended in DMEM/F12 supplemented with 2% FBS. Cells were then centrifuged at 600 × *g* for 5 min. Non-specific binding was blocked using 300 μL of 2% BSA in PBS for 1 hr at 4°C; then the cells were treated for 30 min with 100 μL of solution containing a rabbit anti-rat Lgr5 antibody diluted 1:100 (Abcam). Alexa Fluor 594 mouse anti-rabbit antibody diluted 1:200 was added to the cells for 30 min at room temperature. Cells were washed three times with 1 mL of PBS, resuspended in 500 μL of PBS, and sorted using a flow cytometer.

Lentiviral miR-17 Infection

The immunodeficiency lentiviral system with GFP-expressing miR-17 or lenti-NC (lentivirus expressing negative control miRNAs) was purchased from Hanbio (Shanghai Hanbio). The DE cells were infected with the lentiviral system expressing miR-17 or lenti-NC according to the manufacturer's instructions. FGF2 was added to the medium on the second day when the lentivirus was confirmed to be introduced into the cells. The medium was changed every 2 days.

RNA Extraction, Reverse Transcription, and Real-Time PCR

Total RNA was extracted from the cultured cells using TRIzol Reagent (Ambion) according to the manufacturer's instructions. Relative mRNA expression levels were determined using the SYBR Green method. The sequences of primers are provided in Table S1. All primers were synthesized by GenScript (Nanjing, China). All of the reactions were run in triplicates. After the reactions were complete, the C_T values were determined by setting a fixed threshold. The relative amount of each mRNA was normalized to GAPDH using the equation $2^{-\Delta\Delta CT}$. For miRNA analysis, rat U6 was used to normalize target miRNA expression.

Protein Extraction and Western Blotting

Cells were rinsed with PBS (pH 7.4) and lysed in radioimmunoprecipitation assay (RIPA) lysis buffer (Beyotime, Shanghai, China) with freshly added PMSF (Beyotime, Shanghai, China) for 20 min on ice. Sonication was used to facilitate cell lysis. After centrifugation at 14,000 × *g* at 4°C for 10 min, the supernatants were collected, and the protein concentration was quantified using a bicinchoninic acid (BCA) protein assay kit (Thermo Scientific). The protein levels were quantified by western blotting analysis of the cell extracts using antibodies listed in Table S2.

Immunofluorescence Assays

Cultured cells were washed three times in PBS and then fixed for 15 min in paraformaldehyde (PFA) at room temperature. Then the cells were washed three times in PBS followed by permeabilization and blocking for 1 hr in PBS+0.1% Triton X-100 containing 2% BSA. Primary antibodies were incubated overnight at 4°C. Then the cells were washed with PBS and incubated with secondary antibodies at room temperature for 1 hr. Subsequently, the incubated cells were washed in PBS, and DAPI was used to visualize nuclei. The antibodies and dilutions are listed in Table S2.

Luciferase Assay

The E2F1 or WIF1 3′ UTR containing the predicted target sequence was cloned and inserted into the pMIR-Report plasmid (Ambion) at the SpeI-HindIII site. We also constructed a pMIR-Report plasmid that carried a mutant E2F1 or WIF1 3′ UTR region. 293T cells were cultured in 24-well plates for 24 hr; then each well was transfected with 0.5 μg of firefly luciferase reporter plasmid, 0.3 μg of β-galactosidase expression vector (Ambion), and 15 pmol of miR-17 or miR-NC using Lipofectamine 2000 (Invitrogen). Cells were harvested for the luciferase assay (Promega) 48 hr later, and luciferase activity was normalized to the β-galactosidase activity.

Induction of Experimental Colitis and the Transplantation Experiment

Thirty-seven-week-old male BALB/c mice were randomly assigned into three groups. The first group was the control group, the second group was the sham transplantation group, and the third group was the cell injection group. Acute colitis was induced in the second and third groups by feeding mice 3% DSS (Mpbio) dissolved in drinking water for 7 days. Then on the seventh and ninth days after the start of DSS administration, a total of 150 μL of cell suspension containing 1×10^6 GFP^+ BM-MSC-derived ISCs was transplanted into the third group by enema, whereas an equal amount of PBS was injected into the colons of the second group. After the transplantation, the mice were maintained as usual; then, on day 14, five mice from each group were sacrificed and analyzed. The cell suspension was instilled into the colonic lumen using a 1-mL syringe and a gastric catheter. Mice were anaesthetized using diethyl ether before the injection. The distance between one end of the needle and the anus was 4 cm. After cell injection, the mice were held by the tail in a vertical position for 30 s to ensure that the cell suspension was not ejected. The colon was excised for histopathological analysis, as well as immunofluorescence

and cytokine measurements. Weight loss and bloody stool of mice were monitored daily to evaluate the severity of colitis. Then the rest of the mice were sacrificed 1 month after DSS administration, and colon sections were analyzed by immunofluorescence staining. The animal studies were approved by the Animal Care and Use Committee at Nanjing University. All animal care and handling procedures were performed in accordance with the NIH's *Guide for the Care and Use of Laboratory Animals*.

Cytokine Measurements

Blood was collected after removing the eyeballs. Plasma was obtained following centrifugation 3,000 × *g* for 5 min at room temperature. Cytokine levels were measured using ELISA Kits (BioPlex; Bio-Rad, Segrate, Italy). For tissue inflammatory cytokine analysis, one section of colon (0.5 g) from each mouse was evaluated by qRT-PCR.

Histopathological Analysis

All mice were sacrificed by cervical dislocation, and the colon was excised. The length of each colon was recorded. In addition, the colon was rinsed with PBS, fixed in 4% PFA, and embedded in Optimal Cutting Temperature compound or paraffin wax. Tissue sections were stained with H&E. The Swiss roll technique was used for the immunofluorescence analysis.[41]

Statistical Analysis

Data are presented as the mean ± SEM. Each experiment was performed at least three times. Data were analyzed with Student's t test, the Mann-Whitney test, and the ANOVA F-test. Statistical analysis was performed with GraphPad Prism software version 5.0 (La Jolla, CA, USA). $p < 0.05$ was considered to be statistically significant.

SUPPLEMENTAL INFORMATION

Supplemental Information includes four figures and two tables and can be found with this article online at https://doi.org/10.1016/j.omtn.2018.08.017.

AUTHOR CONTRIBUTIONS

The authors contributed in the following ways: L.Y., L.L., and F.Y.W. designed the experiment; L.Y., L.X.S., M.H.W., J. Wang, L.W., and X.D. conducted the experiment and contributed to analyzing the results; L.Y., L.L., J. Wei, and Y.F.W. wrote the manuscript.

CONFLICTS OF INTEREST

The authors have no conflicts of interest.

ACKNOWLEDGMENTS

The authors thank the research team from the Life Science School of Nanjing University. This work was supported by the National Natural Science Foundation of China (grant 81570506).The foundations providing grants had no role in the study design; collection, analysis, and interpretation of the data; writing of the report; or the decision to submit the paper.

REFERENCES

1. Rutgeerts, P., Vermeire, S., and Van Assche, G. (2007). Mucosal healing in inflammatory bowel disease: impossible ideal or therapeutic target? Gut *56*, 453–455.
2. Zallot, C., and Peyrin-Biroulet, L. (2013). Deep remission in inflammatory bowel disease: looking beyond symptoms. Curr. Gastroenterol. Rep. *15*, 315.
3. Sato, T., Vries, R.G., Snippert, H.J., van de Wetering, M., Barker, N., Stange, D.E., van Es, J.H., Abo, A., Kujala, P., Peters, P.J., and Clevers, H. (2009). Single Lgr5 stem cells build crypt-villus structures in vitro without a mesenchymal niche. Nature *459*, 262–265.
4. Clevers, H. (2013). The intestinal crypt, a prototype stem cell compartment. Cell *154*, 274–284.
5. Barker, N., van Es, J.H., Kuipers, J., Kujala, P., van den Born, M., Cozijnsen, M., Haegebarth, A., Korving, J., Begthel, H., Peters, P.J., and Clevers, H. (2007). Identification of stem cells in small intestine and colon by marker gene Lgr5. Nature *449*, 1003–1007.
6. Sangiorgi, E., and Capecchi, M.R. (2008). Bmi1 is expressed in vivo in intestinal stem cells. Nat. Genet. *40*, 915–920.
7. Kayahara, T., Sawada, M., Takaishi, S., Fukui, H., Seno, H., Fukuzawa, H., Suzuki, K., Hiai, H., Kageyama, R., Okano, H., and Chiba, T. (2003). Candidate markers for stem and early progenitor cells, Musashi-1 and Hes1, are expressed in crypt base columnar cells of mouse small intestine. FEBS Lett. *535*, 131–135.
8. Potten, C.S., Booth, C., Tudor, G.L., Booth, D., Brady, G., Hurley, P., Ashton, G., Clarke, R., Sakakibara, S., and Okano, H. (2003). Identification of a putative intestinal stem cell and early lineage marker; musashi-1. Differentiation *71*, 28–41.
9. Spence, J.R., Mayhew, C.N., Rankin, S.A., Kuhar, M.F., Vallance, J.E., Tolle, K., Hoskins, E.E., Kalinichenko, V.V., Wells, S.I., Zorn, A.M., et al. (2011). Directed differentiation of human pluripotent stem cells into intestinal tissue in vitro. Nature *470*, 105–109.
10. Ogaki, S., Shiraki, N., Kume, K., and Kume, S. (2013). Wnt and Notch signals guide embryonic stem cell differentiation into the intestinal lineages. Stem Cells *31*, 1086–1096.
11. Ogaki, S., Morooka, M., Otera, K., and Kume, S. (2015). A cost-effective system for differentiation of intestinal epithelium from human induced pluripotent stem cells. Sci. Rep. *5*, 17297.
12. Iwao, T., Toyota, M., Miyagawa, Y., Okita, H., Kiyokawa, N., Akutsu, H., Umezawa, A., Nagata, K., and Matsunaga, T. (2014). Differentiation of human induced pluripotent stem cells into functional enterocyte-like cells using a simple method. Drug Metab. Pharmacokinet. *29*, 44–51.
13. Riegler, J., Ebert, A., Qin, X., Shen, Q., Wang, M., Ameen, M., Kodo, K., Ong, S.G., Lee, W.H., Lee, G., et al. (2016). Comparison of magnetic resonance imaging and serum biomarkers for detection of human pluripotent stem cell-derived teratomas. Stem Cell Reports *6*, 176–187.
14. Hass, R., Kasper, C., Bohm, S., and Jacobs, R. (2011). Different populations and sources of human mesenchymal stem cells (MSC): a comparison of adult and neonatal tissue-derived MSC. Cell Commun. Signal *9*, 12.
15. Lanzoni, G., Roda, G., Belluzzi, A., Roda, E., and Bagnara, G.P. (2008). Inflammatory bowel disease: moving toward a stem cell-based therapy. World J. Gastroenterol. *14*, 4616–4626.
16. Eggenhofer, E., Luk, F., Dahlke, M.H., and Hoogduijn, M.J. (2014). The life and fate of mesenchymal stem cells. Front. Immunol. *5*, 148.
17. Figueroa, F.E., Carrión, F., Villanueva, S., and Khoury, M. (2012). Mesenchymal stem cell treatment for autoimmune diseases: a critical review. Biol. Res. *45*, 269–277.
18. D'Amour, K.A., Agulnick, A.D., Eliazer, S., Kelly, O.G., Kroon, E., and Baetge, E.E. (2005). Efficient differentiation of human embryonic stem cells to definitive endoderm. Nat. Biotechnol. *23*, 1534–1541.
19. Li, J., Zhu, L., Qu, X., Li, J., Lin, R., Liao, L., Wang, J., Wang, S., Xu, Q., and Zhao, R.C. (2013). Stepwise differentiation of human adipose-derived mesenchymal stem cells toward definitive endoderm and pancreatic progenitor cells by mimicking pancreatic development in vivo. Stem Cells Dev. *22*, 1576–1587.
20. Grapin-Botton, A., and Melton, D.A. (2000). Endoderm development: from patterning to organogenesis. Trends Genet. *16*, 124–130.

21. Dessimoz, J., Opoka, R., Kordich, J.J., Grapin-Botton, A., and Wells, J.M. (2006). FGF signaling is necessary for establishing gut tube domains along the anterior-posterior axis in vivo. Mech. Dev. *123*, 42–55.

22. Ang, S.L., Wierda, A., Wong, D., Stevens, K.A., Cascio, S., Rossant, J., and Zaret, K.S. (1993). The formation and maintenance of the definitive endoderm lineage in the mouse: involvement of HNF3/forkhead proteins. Development *119*, 1301–1315.

23. Silberg, D.G., Swain, G.P., Suh, E.R., and Traber, P.G. (2000). Cdx1 and cdx2 expression during intestinal development. Gastroenterology *119*, 961–971.

24. Ameri, J., Ståhlberg, A., Pedersen, J., Johansson, J.K., Johannesson, M.M., Artner, I., and Semb, H. (2010). FGF2 specifies hESC-derived definitive endoderm into foregut/midgut cell lineages in a concentration-dependent manner. Stem Cells *28*, 45–56.

25. Monzo, M., Navarro, A., Bandres, E., Artells, R., Moreno, I., Gel, B., Ibeas, R., Moreno, J., Martinez, F., Diaz, T., et al. (2008). Overlapping expression of microRNAs in human embryonic colon and colorectal cancer. Cell Res. *18*, 823–833.

26. Li, F., He, Z., Li, Y., Liu, P., Chen, F., Wang, M., Zhu, H., Ding, X., Wangensteen, K.J., Hu, Y., and Wang, X. (2011). Combined activin A/LiCl/Noggin treatment improves production of mouse embryonic stem cell-derived definitive endoderm cells. J. Cell. Biochem. *112*, 1022–1034.

27. Cordero, J.B., and Sansom, O.J. (2012). Wnt signalling and its role in stem cell-driven intestinal regeneration and hyperplasia. Acta Physiol. (Oxf.) *204*, 137–143.

28. Valenta, T., Degirmenci, B., Moor, A.E., Herr, P., Zimmerli, D., Moor, M.B., Hausmann, G., Cantù, C., Aguet, M., and Basler, K. (2016). Wnt ligands secreted by subepithelial mesenchymal cells are essential for the survival of intestinal stem cells and gut homeostasis. Cell Rep. *15*, 911–918.

29. Wu, Z., Zheng, S., Li, Z., Tan, J., and Yu, Q. (2011). E2F1 suppresses Wnt/β-catenin activity through transactivation of β-catenin interacting protein ICAT. Oncogene *30*, 3979–3984.

30. Yu, F., Lu, Z., Huang, K., Wang, X., Xu, Z., Chen, B., Dong, P., and Zheng, J. (2016). MicroRNA-17-5p-activated Wnt/β-catenin pathway contributes to the progression of liver fibrosis. Oncotarget *7*, 81–93.

31. Wirtz, S., Neufert, C., Weigmann, B., and Neurath, M.F. (2007). Chemically induced mouse models of intestinal inflammation. Nat. Protoc. *2*, 541–546.

32. Hayashita, Y., Osada, H., Tatematsu, Y., Yamada, H., Yanagisawa, K., Tomida, S., Yatabe, Y., Kawahara, K., Sekido, Y., and Takahashi, T. (2005). A polycistronic microRNA cluster, miR-17-92, is overexpressed in human lung cancers and enhances cell proliferation. Cancer Res. *65*, 9628–9632.

33. Wang, M., Gu, H., Wang, S., Qian, H., Zhu, W., Zhang, L., Zhao, C., Tao, Y., and Xu, W. (2012). Circulating miR-17-5p and miR-20a: molecular markers for gastric cancer. Mol. Med. Rep. *5*, 1514–1520.

34. Shan, S.W., Fang, L., Shatseva, T., Rutnam, Z.J., Yang, X., Du, W., Lu, W.Y., Xuan, J.W., Deng, Z., and Yang, B.B. (2013). Mature miR-17-5p and passenger miR-17-3p induce hepatocellular carcinoma by targeting PTEN, GalNT7 and vimentin in different signal pathways. J. Cell Sci. *126*, 1517–1530.

35. Mao, S., Li, X., Wang, J., Ding, X., Zhang, C., and Li, L. (2016). miR-17-92 facilitates neuronal differentiation of transplanted neural stem/precursor cells under neuroinflammatory conditions. J. Neuroinflammation *13*, 208.

36. An, X., Ma, K., Zhang, Z., Zhao, T., Zhang, X., Tang, B., and Li, Z. (2016). miR-17, miR-21, and miR-143 enhance adipogenic differentiation from porcine bone marrow-derived mesenchymal stem cells. DNA Cell Biol. *35*, 410–416.

37. Altuvia, Y., Landgraf, P., Lithwick, G., Elefant, N., Pfeffer, S., Aravin, A., Brownstein, M.J., Tuschl, T., and Margalit, H. (2005). Clustering and conservation patterns of human microRNAs. Nucleic Acids Res. *33*, 2697–2706.

38. Khuu, C., Utheim, T.P., and Sehic, A. (2016). The three paralogous microRNA clusters in development and disease, miR-17-92, miR-106a-363, and miR-106b-25. Scientifica (Cairo) *2016*, 1379643.

39. Djouad, F., Plence, P., Bony, C., Tropel, P., Apparailly, F., Sany, J., Noël, D., and Jorgensen, C. (2003). Immunosuppressive effect of mesenchymal stem cells favors tumor growth in allogeneic animals. Blood *102*, 3837–3844.

40. von Bahr, L., Sundberg, B., Lönnies, L., Sander, B., Karbach, H., Hägglund, H., Ljungman, P., Gustafsson, B., Karlsson, H., Le Blanc, K., and Ringdén, O. (2012). Long-term complications, immunologic effects, and role of passage for outcome in mesenchymal stromal cell therapy. Biol. Blood Marrow Transplant. *18*, 557–564.

41. Williams, J.M., Duckworth, C.A., Vowell, K., Burkitt, M.D., and Pritchard, D.M. (2016). Intestinal preparation techniques for histological analysis in the mouse. Curr. Protoc. Mouse Biol. *6*, 148–168.

OMTN, Volume *13*

Supplemental Information

A Simple System for Differentiation of Functional Intestinal Stem Cell-like Cells from Bone Marrow Mesenchymal Stem Cells

Lei Ye, Lei X. Sun, Min H. Wu, Jin Wang, Xin Ding, Hui Shi, Sheng L. Lu, Lin Wu, Juan Wei, Liang Li, and Yu F. Wang

Supplementary Information

A simple system for differentiation of functional intestinal stem cell-like cells from bone marrow mesenchymal stem cells

L Ye[1+], XL Sun[2+], HM Wu[1], J Wang[2], X Ding[2], H Shi[1], LS Lu[2],L Wu[1], J Wei[1], L Li[2*], FY Wang[1*]

Figure S1. Systemic inflammatory response as reflected by plasma cytokine levels measured by ELISA. Data are shown as the mean±standard error of the mean; n=5, * P<0.05, and ** P<0.01. INF-γ, interferon gamma; IL, interleukin; TNF-a, tumournecrosis factor alpha.

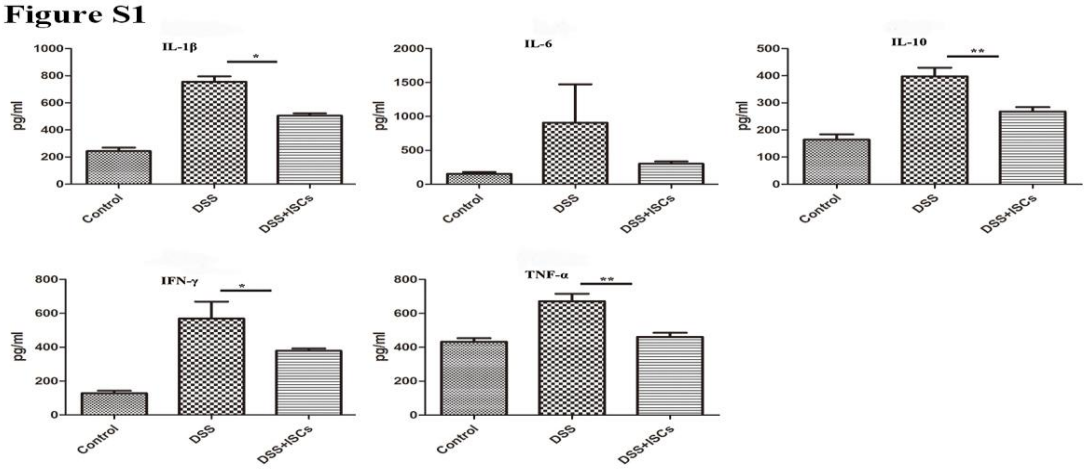

Figure S2. Seven days after transplantation, the colon swiss roll technique showed that the GFP$^+$ area was concentrated in the middle and lower parts of the colon. Nuclei were stained with DAPI. Scale bar: 12.5μm.

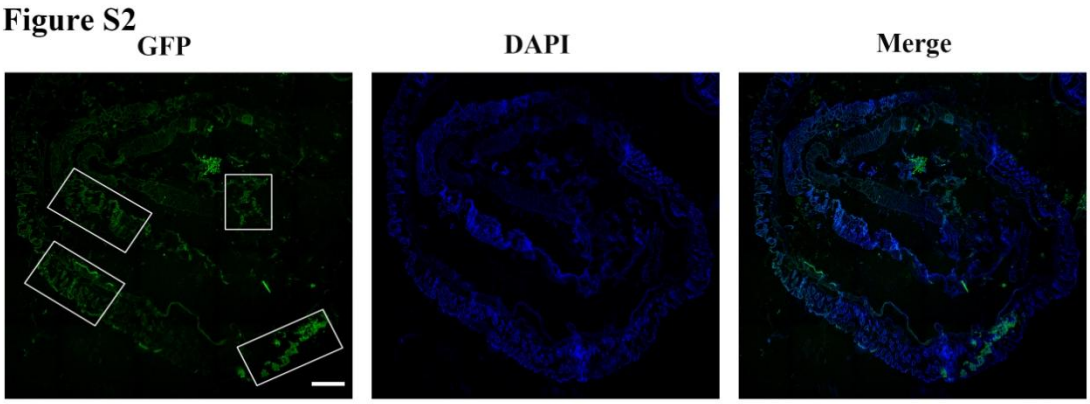

Figure S3. High-powered views of the GFP^{+} cystic structures. Nuclei were stained with DAPI. Scale bar: 50μm.

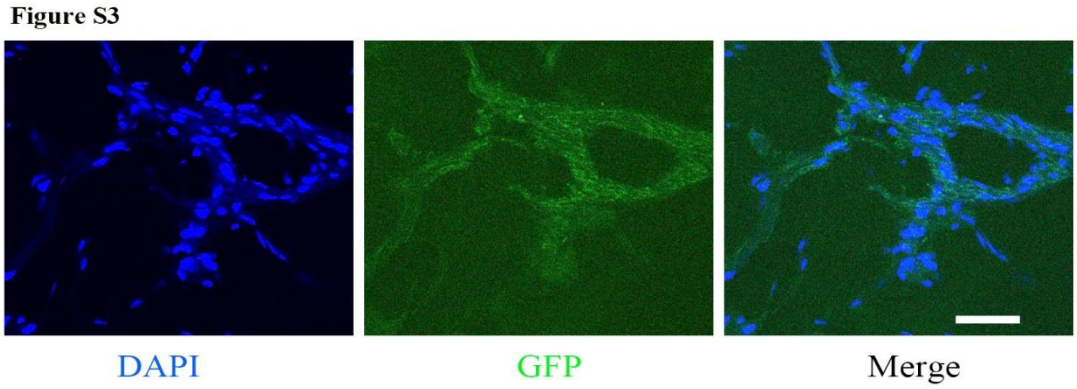

Figure S4. The migration process of the engrafted cells. Nuclei were stained with DAPI. Scale bar: 75μm.

Figure S4

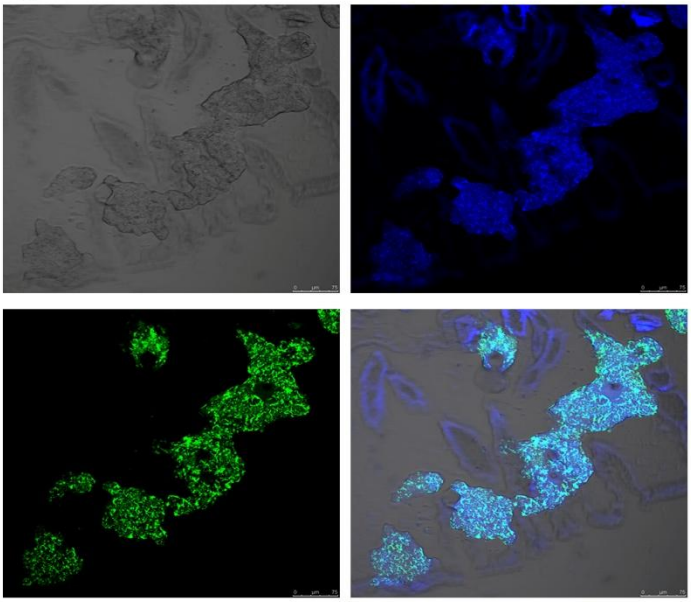

Supplementary Table 1 Primers used in the study

Name	Sequence 5'—3'
Sox17-F	TCTGACGGTTGCCGATTT
Sox17-R	CTGGACAGTGATGGTGGG
Foxa2-F	CAGTGGCGGAGGCAAGAAGAC
Foxa2-R	CTCAGCGCAGAGGCAGGTGTT
Lgr5-F	AATGCCATACGCTTACCA
Lgr5-R	TCTTCAAGGTCCCGCTCA
Musashi-1-F	TACAGCCATCCCTCTCACTG
Musashi-1-R	GCTGGGAGTAGAACCTGGAG
(rat)GAPDH-F	CCTGGAGAAACCTGCCAG
(rat)GAPDH-R	CACAGGAGACAACCTGGTCC
WIF1-F	TGGCATGGGAGACACTGCAA
WIF1-R	AGGCTGTGAACTCGGCGTAA
E2F1-F	CTCTGAAGCAAGGGCAGGGT
E2F1-R	ATCAGCCAAGGCCCTCACTC
β-catenin-F	TACCGAGCCTGCCATCTGTG
β-catenin-R	TTTGCTGGGCAAAGGGCAAG
ISX-F	TACCCAGAGCTTGCCATTA
ISX-R	CATCCCAGCCCTTAGTCA
Villin 1-F	AAAGCCAAGCAGTACCCACCTAG
Villin 1-R	CATCAAACTTCACCTGTTCCACC
DDP4-F	CGGAATAAATGACTGGG
DDP4-R	TTGCATGGGAATCGTAG
IFN-γ-F	GGATGGTGACATGAAAATCCTGC
IFN-γ-R	TGCTGATGGCCTGATTGTCTT
IL-10-F	GCTCTTACTGACTGGCATGAG
IL-10-R	CGCAGCTCTAGGAGCATGTG
IL-6-F	TAGTCCTTCCTACCCCAATTTCC
IL-6-R	TTGGTCCTTAGCCACTCCTTC
TNF-a-F	CCCTCACACTCAGATCATCTTCT
TNF-a-R	GCTACGACGTGGGCTACAG
(mouse)GAPDH-F	AGGTCGGTGTGAACGGATTTG
(mouse)GAPDH-R	TGTAGACCATGTAGTTGAGGTCA

Supplementary Table 2 Primary antibodies used in the study

Primary antibodies for Western blot

Name	Company	Catalog no.	Dilution
Sox17	Abcam	ab191699	1:1000
Foxa2	CST	8186p	1:1000
Lgr5	Abcam	ab75850	1:1000
Musashi-1	Novus	NB100-1759	1:500
WIF1	absin	abs116623	1:1000
E2F1	Abcam	ab179445	1:1000
β -catenin	CST	8480p	1:1000
β -catenin(phospho Y142)	Abcam	ab27798	1:1000
GAPDH	Santa Cruz	sc32233	1:2000

Primary antibodies for immunofluorescence assay

Name	Company	Catalog no.	Dilution
Sox17	Abcam	ab191699	1:50
Foxa2	Abcam	ab108396	1:100
Lgr5	absin	abs106134	1:50
Musashi-1	Novus	NB100-1759	1:20
E-cadherin	Abcam	ab40772	1:100
MUC2	Abcam	ab76774	1:300
CK-18	Abcam	ab133263	1:100
Phalloidin	Yeasen	40735ES75	1:200